



Published in final edited form as:

Cell Rep. 2015 September 01; 12(9): 1456–1470. doi:10.1016/j.celrep.2015.07.053.

## PRC2 is required to maintain expression of the maternal *Gtl2-Rian-Mirg* locus by preventing *de novo* DNA methylation in mouse embryonic stem cells

Partha Pratim Das<sup>1,2,16</sup>, David A. Hendrix<sup>3,4,16</sup>, Effie Apostolou<sup>5,6,7</sup>, Alice H. Buchner<sup>1,8</sup>, Matthew C. Canver<sup>1</sup>, Semir Beyaz<sup>1</sup>, Damir Ljuboja<sup>1</sup>, Rachael Kuintzle<sup>4</sup>, Woojin Kim<sup>1</sup>, Rahul Karnik<sup>5,9</sup>, Zhen Shao<sup>1,10</sup>, Huafeng Xie<sup>1</sup>, Jian Xu<sup>1,11</sup>, Alejandro De Los Angeles<sup>1</sup>, Yingying Zhang<sup>5,9</sup>, Junho Choe<sup>12</sup>, Don Leong Jia Jun<sup>1,13</sup>, Xiaohua Shen<sup>1,14</sup>, Richard I. Gregory<sup>12</sup>, George Q. Daley<sup>1,2</sup>, Alexander Meissner<sup>5,9</sup>, Manolis Kellis<sup>3</sup>, Konrad Hochedlinger<sup>5,6,2</sup>, Jonghwan Kim<sup>1,15</sup>, and Stuart H. Orkin<sup>1,2,\*</sup>

<sup>1</sup>Division of Hematology/Oncology, Boston Children's Hospital and Department of Pediatric Oncology, Dana-Farber Cancer Institute, Harvard Stem Cell Institute, Harvard Medical School, Boston, MA 02115, USA

<sup>2</sup>Howard Hughes Medical Institute, Boston, MA 02115, USA

<sup>3</sup>Computer Science and Artificial Intelligence Laboratory, Massachusetts Institute of Technology (MIT), Cambridge, Massachusetts 02139, USA

<sup>5</sup>Department of Stem Cell and Regenerative Biology, Harvard University and Harvard Medical School, 7 Divinity Avenue, Cambridge, MA 02138

<sup>6</sup>Massachusetts General Hospital Cancer Center and Center for Regenerative Medicine, Boston, MA 02114

<sup>7</sup>Department of Medicine and Cancer Center, Weill Cornell Medical College, Belfer Research Building, 413 East 69th Street, New York, NY 10021

<sup>8</sup>Internaitonal Max Planck Research School, Molecular Biology Program, Georg-August-Universität Göttingen, Justus-von-Liebig-Weg 11, 37077 Göttingen, Germany

\*Correspondence: stuart\_orkin@dfci.harvard.edu (S.H.O.).

<sup>4</sup>Present address: Department of Biochemistry and Biophysics, School of Electrical Engineering and Computer Science, Oregon State University, 2011 Ag and Life Science Bldg, Corvallis, OR 97331-7305

<sup>10</sup>Present address: Key Laboratory of Computational Biology, CAS-MPG Partner Institute for Computational Biology, Shanghai Institutes for Biological Sciences, Chinese Academy of Sciences, Shanghai 200031, China

<sup>14</sup>Present address: Tsinghua-Peking Center for Life Sciences, School of Medicine, Tsinghua University, Beijing, 100084, China

<sup>15</sup>Present address: Department of Molecular Biosciences, Institute for Cellular and Molecular Biology, Center for Systems and Synthetic Biology, The University of Texas at Austin, Austin, Texas

<sup>16</sup>These authors contributed equally to this work

### ACCESSION NUMBERS

RNA-Seq, small RNA-Seq, ChIP-Seq and microarray data have been deposited in the Gene Expression Omnibus (GEO) under accession number GSE58414.

### SUPPLEMENTAL INFORMATION

Supplemental information for this article includes five Figures, eight tables and experimental procedures.

### AUTHOR CONTRIBUTIONS

P.P.D. and S.H.O. designed the experiments; P.P.D., E.A., A.H.B., S.B., D.L., H.X., D.L.J.J., M.C.C., J.C., J.X., Y.Z., W.K., A.D.L.A. and X.S. performed the experiments; P.P.D., D.A.H., R.K. and Z.S. analyzed the data; P.P.D., D.A.H., A.M., K.H., M.K., G.Q.D., R.I.G., J.K. and S.H.O. interpreted the data; P.P.D., D.A.H. and S.H.O. wrote the manuscript.

<sup>9</sup>Broad Institute, Cambridge, Massachusetts 02142, USA

<sup>11</sup>Children's Medical Center Research Institute and Department of Pediatrics, The University of Texas Southwestern Medical Center, Dallas, TX, USA 75235

<sup>12</sup>Stem Cell Program, Boston Children's Hospital, Department of Biological Chemistry and Molecular Pharmacology and Department of Pediatrics, Harvard Medical School, Harvard Stem Cell Institute, Boston, MA 02115, USA

<sup>13</sup>School of Chemical and Life Sciences, Singapore Polytechnic, 500 Dover Road, Singapore 139651

## SUMMARY

Polycomb Repressive Complex 2 (PRC2) function and DNA methylation (DNAm) are typically correlated with the gene repression. Here, we show that PRC2 is required to maintain expression of maternal microRNAs (miRNAs) and long non-coding RNAs (lncRNAs) from the *Gtl2-Rian-Mirg* locus, which is essential for full pluripotency of iPSCs. In the absence of PRC2 the entire locus becomes transcriptionally repressed due to gain of DNA methylation at the intergenic differentially methylated regions (IG-DMR). Furthermore, we demonstrate that the IG-DMR serves as an enhancer of the maternal *Gtl2-Rian-Mirg* locus. Mechanistic study reveals that PRC2 interacts physically with Dnmt3 methyltransferases and prevents their recruitment and subsequent DNAm at the IG-DMR, thereby allowing for proper expression of the maternal *Gtl2-Rian-Mirg* locus. Our observations provide a novel mechanism by which PRC2 counteracts the action of Dnmt3 methyltransferases at an imprinted locus required for full pluripotency.

## INTRODUCTION

Somatic cells are readily converted to an ESC-like state (induced pluripotent cells, iPSCs) through enforced expression of a defined set of transcription factors, including Oct4, Sox2, Klf4 and c-Myc (OSKM) (Takahashi and Yamanaka, 2006). However, it remains unclear whether iPSCs are molecularly and functionally equivalent to blastocyst-derived embryonic stem cells (ESCs). Overall messenger RNA (mRNA) and microRNA (miRNA) expression patterns are nearly indistinguishable between genetically matched mouse ESCs and iPSCs, with the exception of a few maternally expressed long non-coding RNAs (*Gtl2*, *Rian* and *Mirg*) and miRNAs originating from the imprinted *Dlk1-Dio3* gene cluster that is “silenced” in the majority of iPSC clones (Stadtfeld et al., 2010). iPSC clones with a silenced *Dlk1-Dio3* gene cluster (called *Gtl2<sup>OFF</sup>* clones) poorly contribute to chimeras and fail to yield viable iPSCs-derived mice (all-iPSC mice). In contrast, iPSC clones with proper expression of the *Dlk1-Dio3* gene cluster (called *Gtl2<sup>ON</sup>* clones) contribute to high grade of chimeras and generate viable all-iPSC mice (Stadtfeld et al., 2010). Moreover, ascorbic acid (Vitamin C) prevents loss of imprinting at *Dlk1-Dio3* gene cluster and facilitates generation of all-iPSC mice from differentiated B-cells (Stadtfeld et al., 2012). Thus, expression of maternal lncRNAs and miRNAs from the *Dlk1-Dio3* imprinted gene cluster is essential for establishment of full pluripotency. We have found unexpectedly that Polycomb Repressive Complex-2 (PRC2) is required to maintain expression of the *Dlk1-Dio3* imprinted gene cluster, and that PRC2 counteracts *de novo* DNA methylation at this locus.

PRC2, which is comprised of the core components Ezh2/Ezh1, Eed, Suz12, histone chaperones Rbbp4/6, and associated other factors (e.g. Pcl1 and Jarid2), catalyzes H3K27me<sub>2/3</sub>, a chromatin mark correlated with transcriptional repression at silent and bivalent genes (Margueron and Reinberg, 2011). In embryonic stem cells (ESCs), many PRC2 targets are bivalent and marked by both H3K4me<sub>3</sub> and H3K27me<sub>3</sub> at lineage-specific genes that are “poised,” but activated upon differentiation (Boyer et al., 2006). As such, PRC2 is critical for both ESC maintenance and differentiation. Although bivalent domains were initially believed to be ESC-specific, they have been identified in differentiated somatic cells at lower frequency (Bernstein et al., 2006; Mikkelsen et al., 2007). While most functions of PRC2 correlate with repression, a minority of studies implicate PRC2 in active transcription at a subset of its target genes in mESCs (Brookes et al., 2012; Ferrari et al., 2014).

The mechanism by which PRC2 is recruited to its target genes is incompletely understood. In *Drosophila*, Polycomb response elements (PRE) are responsible for PRC2 recruitment (Simon and Kingston, 2009). However, in mammals this is not the case. Instead, PRC2 is recruited at highly enriched CpG islands (Ku et al., 2008). Recent findings also posit that long non-coding RNAs (lncRNAs) are important for PRC2 recruitment and its function. In mammals, X-chromosome inactivation (XCI) initiates expression of the ~17kb long non-coding RNA Xist, which binds to PRC2 and catalyzes H3K27me<sub>3</sub> in *-cis* to control chromosome-wide silencing (Zhao et al., 2008). Also, repression of the *Hox-D* locus appears to be regulated in *-trans* by Hotair that is generated from *Hox-C* locus and binds to PRC2 (Rinn et al., 2007). In addition, a class of short RNAs (50–200nt) plays an important role in association with PRC2 to regulate its target genes (Kanhere et al., 2010). Genome-wide analysis using RNA immunoprecipitation-sequencing (RIP) demonstrates >9000 lncRNAs (>200nt in size) are associated with PRC2 (Zhao et al., 2010). The PRC2-interacting transcriptome consists of numerous transcripts, such as Xist, H19, Igf2, Air, Igf2r, Kcnq1 and Gtl2, that originate from genomic imprinted loci (Zhao et al., 2010). Genomic imprinting is an epigenetic phenomenon in which genes are expressed either from the paternally or maternally inherited allele (Edwards and Ferguson-Smith, 2007). The majority of imprinted genes are clustered in the genome, and usually contain protein coding genes as well as at least one non-coding RNA (ncRNA) (Edwards and Ferguson-Smith, 2007). Each cluster is under the control of a *cis*-regulatory element, termed the imprinting control region (ICR). ICRs generally acquire DNA methylation during oogenesis or spermatogenesis in germ cells and that leads to imprinting of one of the parental alleles (Rocha et al., 2008). The detailed functions of PRC2-lncRNAs in mediating the regulation of genomic imprinting are largely unknown. For example, PRC2-Gtl2 lncRNA represses *Dlk1* expression in *-cis* (Zhao et al., 2010); similarly, Kcnq1ot1 lncRNA interacts with PRC2 and silences genes in the *Kcnq1* domain in *-cis* (Pandey et al., 2008).

Contrary to the conventional role of PRC2 in maintenance of repression, we demonstrate here that PRC2 is required to maintain expression of maternal microRNAs (miRNAs) and long non-coding RNAs (lncRNAs) from the *Gtl2-Rian-Mirg* locus within the *Dlk1-Dio3* imprinted gene cluster in mouse ESCs. In the absence of Ezh2/PRC2, the entire *Gtl2-Rian-Mirg* locus becomes transcriptionally silent due to gain of *de novo* DNA methylation at the IG-DMR, a critical *cis*-regulatory element that controls expression of maternal *Gtl2-Rian-*

*Mirg* locus. In the presence of PRC2, the maternal IG-DMR is lowly methylated and acts as an enhancer of the maternal *Gtl2-Rian-Mirg* locus. Further mechanistic study shows that PRC2 prevents Dnmt3 methyltransferases recruitment and subsequent *de novo* DNAm at the IG-DMR, thereby allowing proper expression of the maternal *Gtl2-Rian-Mirg* locus. These findings reveal an unanticipated function of PRC2, as well as the complex interplay between PRC2 function and DNA methylation. Our observations provide a novel mechanism by which PRC2 antagonizes *de novo* DNAm at an imprinted locus.

## RESULTS

### PRC2 is required to maintain expression of maternal miRNAs and lncRNAs at the *Gtl2-Rian-Mirg* locus

To further investigate the role of PRC2 in gene regulation in mESCs, we conducted both RNA and size-selected small RNA expression profiling using high-throughput sequencing of *Ezh2*<sup>-/-</sup> and wild-type mESCs. We observed striking reduction of expression of a cluster of microRNAs (miRNAs) in *Ezh2*<sup>-/-</sup> mESCs at the *Gtl2-Rian-Mirg* locus within the *Dlk1-Dio3* imprinted gene cluster on chromosome 12qf1 (Figures 1A–1B). The *Gtl2-Rian-Mirg* locus harbors lncRNA genes (*Gtl2*, *Rian* and *Mirg*), miRNAs, and snoRNAs that are expressed from the maternally inherited chromosome; whereas protein coding genes *Dlk1* and *Dio3* are expressed from the paternally inherited chromosome (Figure 1B) (Rocha et al., 2008). Furthermore, global RT-qPCR analysis of total miRNA expression per chromosome revealed significant reduction of miRNA expression from chromosome 12 in *Ezh2*<sup>-/-</sup> mESCs (Figure S1B), as the majority of the miRNAs reside at the maternal *Gtl2-Rian-Mirg* locus of chromosome 12. We also observed reduced expression of maternal miRNAs derived from the *Gtl2-Rian-Mirg* locus, as well as from chromosome 12, in *Eed*<sup>-/-</sup> and *Jarid2*<sup>-/-</sup> mESCs (Figures S1A–S1B). Northern blot and quantitative RT-qPCR confirmed reduced expression of selected maternal miRNAs (miR-127, miR-134, miR-323-3p, miR-410, miR-431 and miR-433) in *Ezh2*<sup>-/-</sup>, as well as in *Eed*<sup>-/-</sup> and *Jarid2*<sup>-/-</sup> mESCs as compared to wild-type (Figure 1C, & S1C–S1E). Another independent *Ezh2*<sup>-/-</sup> clone showed similar level of reduction of all these maternal miRNAs (Figure S1H). To exclude possible effects on miRNA biogenesis in the absence of PRC2, we examined expression of Dicer, Drosha, and Ago2. Expression of these critical factors for miRNA biogenesis was unchanged in the absence of PRC2 (Figures S1F).

Next, we examined expression of lncRNAs-*Gtl2* (also known as *Meg3*), *Rian* and *Mirg*, as well as protein coding genes *Dlk1* and *Dio3*. RNA-seq and RT-qPCR revealed marked reduction of expression of the maternal *Gtl2*, *Rian* and *Mirg* lncRNAs in two independent *Ezh2*<sup>-/-</sup> mESCs clones, similar to the observed deficit in miRNAs expression in these cells. However, expression of the paternal *Dlk1* and *Dio3* alleles was unaffected (Figures 1D, S1G and S1I). Similarly, expression of *Gtl2*, *Rian* and *Mirg* lncRNAs was also reduced in *Eed*<sup>-/-</sup> and *Jarid2*<sup>-/-</sup> mESCs (Figures S1G and S1J). The deficit in expression of miRNAs and lncRNAs was greater in the absence of *Ezh2* as compared to *Eed* or *Jarid2* loss. Marked reduction of expression of maternal miRNAs and lncRNAs from the *Gtl2-Rian-Mirg* locus in the absence of several PRC2 components implies that transcription of the entire locus was affected in absence of intact PRC2. To establish this, we performed CHIP-seq analysis of

RNA Pol II, which revealed significant reduction of RNA Pol II occupancy at the entire *Gtl2-Rian-Mirg* locus (~220kb) in *Ezh2*<sup>-/-</sup> mESCs, as compared to wild-type (Figure 1E). Thus, the entire maternal *Gtl2-Rian-Mirg* locus is repressed in the absence of Ezh2/PRC2. Interestingly, RNA Pol II co-occupied with H3K36me3 and H3K79me2 elongation marks at the *Gtl2-Rian-Mirg* locus (Zhou et al., 2010) (Figure 1E). This continuous stretch of co-occupancy of RNA Pol II, H3K36me3, H3K79me2 and sense-strand specificity of maternal miRNAs and lncRNAs indicates that the maternal *Gtl2-Rian-Mirg* locus may acts as a single transcriptional unit; and most likely maternal miRNAs and lncRNAs are processed from this single transcript. Moreover, a global view of mRNA expression analysis of all imprinted genes showed differential expression of selected imprinted genes in the absence of PRC2 components (Figure S1K). Most pronounced reduction in expression was observed at the *Gtl2-Rian-Mirg* locus in the absence of Ezh2, Eed and Jarid2 of the PRC2 components; H19 expression was significantly reduced, but only in the absence of Ezh2 or Jarid2 (Figures S1K–S1L).

### Methylation of the *Gtl2-Rian-Mirg* locus in the absence of PRC2

To explore mechanisms by which PRC2 loss might lead to repression of the *Gtl2-Rian-Mirg* locus, we first attempted to rescue Ezh2 expression in *Ezh2*<sup>-/-</sup> mESCs. Individual Ezh2 rescue clones expressing different levels of exogenous Ezh2 were examined (Figures S2A and S2C). Ezh2 rescue clones with low level Ezh2 expression failed to rescue expression of maternal lncRNAs and miRNAs (Figures 2A–2B). Even Ezh2 rescue clones (clones A5 and B6) that expressed at near endogenous level of Ezh2 and restore global H3K27me3, failed to rescue maternal Gtl2, Rian and Mirg lncRNAs, as well as miRNAs expression from the *Gtl2-Rian-Mirg* locus (Figures 2A–2B and Figures S2B–S2E). To explore the basis for highly inefficient rescue of maternal lncRNAs and miRNAs upon re-expression of Ezh2, we assessed DNA methylation (DNAm) level at the IG-DMR region, an important regulatory element located ~12kb upstream of the *Gtl2* promoter involved in regional imprinting at the *Gtl2-Rian-Mirg* locus. The IG-DMR of the paternally inherited chromosome was heavily methylated. In contrast, the IG-DMR on the maternally inherited chromosome remained unmethylated (Figure 1B) (Lin et al., 2003; Rocha et al., 2008). As expected, the IG-DMR was 45% DNA methylated in wild-type mESCs. However, the methylation level increased to 92% in *Ezh2*<sup>-/-</sup> mESCs. Ezh2 rescued clones A5 and B6, which expressed near endogenous levels of Ezh2, retained 92% and 88% DNAm at the IG-DMR, respectively (Figure 2C). Furthermore, treatment with high concentrations of the Dnmt inhibitor 5-azacitidine (5-aza) failed to restore Gtl2 expression in *Ezh2*<sup>-/-</sup> mESCs and Ezh2 rescued clones (Figure S2F). Similarly, high concentrations of ascorbic acid (vitamin C) failed to restore Gtl2 expression in *Ezh2*<sup>-/-</sup> (Figure S2G). Thus, DNAm at the IG-DMR is both dense and stable in the absence of Ezh2. Moreover, we observed a small increase in H3K9me3 occupancy at the IG-DMR locus in *Ezh2*<sup>-/-</sup> mESCs as compared to wild-type (Figure S2H), suggesting that cooperation between DNA methylation and H3K9me3 may lead to stable and long-term silencing of the maternal *Gtl2-Rian-Mirg* locus (Epsztejn-Litman et al., 2008; Dong et al., 2008; Smith and Meissner, 2013) in the absence of Ezh2. These data imply that DNA methylation (DNAm) is stable at the IG-DMR in absence of Ezh2, and causes repression of lncRNAs and miRNAs. Once DNAm is established, re-expression of Ezh2 is unable to erase DNAm from the IG-DMR. Taken together, these results indicate that PRC2 is



required to maintain expression of the maternal *Gtl2-Rian-Mirg* locus, most likely through preventing DNAm at the IG-DMR.

### IG-DMR/Enhancer1 serves as an enhancer for the *Gtl2-Rian-Mirg* locus

DNAm at the IG-DMR has been established as essential for proper imprinting control (Lin et al., 2003; Rocha et al., 2008). However, the role of histone modifications at the IG-DMR in imprinting is less well understood. We examined the binding landscape of ESC-specific pluripotency factors, cohesion, mediators, histone marks and PRC2 components at the entire *Dlk1-Dio3* gene cluster (Figure 3A and Figure S3A). The IG-DMR region was co-occupied by ESC-specific transcription factors (TFs) (e.g. Oct4, Nanog, Sox2, Klf4, Esrrb), mediator (Med1/12), cohesin (Smc1/3), Lsd1, H3K27ac and H3K4me1 (Figures 3A–3C). Taken together, these characteristics are consistent with this region serving as an enhancer (Kagey et al., 2010; Whyte et al., 2012). We designate this region Enhancer1 (Enh1). A similar region (Enhancer2, Enh2), located farther downstream (~450kb) of Enh1, showed similar binding patterns (Figure 3D). Both Enh1 and Enh2 exhibited strong enhancer activity in reporter assays (Figure 3E). Interestingly, we observed that the H3K27ac mark was significantly reduced at Enh1 and Enh2 in *Ezh2*<sup>-/-</sup> mESCs. This finding correlates with reduced expression of maternal lncRNAs and miRNAs from the *Gtl2-Rian-Mirg* locus in the absence of *Ezh2*, suggesting that the H3K27ac active histone mark is an indicator of transcription activity of this imprinted locus (Figure 3C–3D) (Xie et al., 2012). Of note, we observed reduced marking with H3K27ac and H3K4me3, as well at the *Gtl2* promoter in the absence of *Ezh2*/ PRC2. Strikingly, we found weak occupancy of *Ezh2*, *Jarid2* and no binding of *Suz12* of PRC2 components at IG-DMR/Enh1 and Enh2, and failed to observe detectable H3K27me3 deposition (Figure 3C–3D). We cannot exclude the possibility that weak binding of *Ezh2*/ PRC2 that is seen derives from the paternal allele.

The similarities between Enh1 and Enh2 led us to consider how together they might regulate the maternal *Gtl2-Rian-Mirg* locus. However, unlike IG-DMR/Enh1, Enh2 is not hypermethylated in absence of *Ezh2* (Figure S3B). We investigated whether Enh1 and Enh2 loop into proximity with the *Gtl2* promoter to regulate the *Gtl2-Rian-Mirg* locus. Chromosomal conformation capture (3C) revealed that both Enh1 and Enh2 interact with the *Gtl2* promoter in the presence and absence of *Ezh2* (Figure S3C), suggesting that *Ezh2* does not interfere with looping between *Gtl2* promoter and Enh1, Enh2. To determine a requirement for IG-DMR/Enh1 and Enh2 in regulation of the *Gtl2-Rian-Mirg* locus, we deleted Enh1 (7kb) and Enh2 (7kb) using the clustered regularly interspaced short palindromic repeats (CRISPR)/Cas9 nuclease system (Cong et al., 2013). Biallelic deletion of Enh2 (*Enh2*<sup>-/-</sup>) failed to affect expression of the *Gtl2-Rian-Mirg* locus. In contrast, biallelic deletion of IG-DMR/Enh1 (*IG-DMR/Enh1*<sup>-/-</sup>) abrogated expression of maternal *Gtl2*, *Rian* and *Mirg* (Figure 3F), demonstrating that IG-DMR/Enh1 is an essential regulatory element for the maternal *Gtl2-Rian-Mirg* locus (Lin et al., 2003). We identified strong co-occupancy of PRC2 and H3K27me3 at the *Dlk1* promoter (Figures 3A–3B). Therefore, we hypothesized that PRC2 might distally regulate the *Gtl2-Rian-Mirg* locus. To test this possibility, we deleted the *Dlk1* promoter region (3kb) using CRISPR/Cas9. Biallelic deletion of the *Dlk1* promoter showed no effect on the locus (Figure S3D), indicating that PRC2 does not distally regulate the *Gtl2-Rian-Mirg* locus. Collectively, these

results demonstrate that the IG-DMR/Enh1 is an important cis-regulatory element that serves as an enhancer for the maternal *Gtl2-Rian-Mirg* locus.

### **PRC2 physically interacts with Dnmt3a/3l in Gtl2 lncRNA-independent manner, and the interaction between Gtl2 lncRNA-Ezh2 inhibits binding of Ezh2/PRC2 at the IG-DMR**

Our results demonstrate that in the absence of PRC2 the entire maternal *Gtl2-Rian-Mirg* locus is transcriptionally repressed in association with DNA hypermethylation at the IG-DMR (Figures 1 and 2). These data hint at a strong connection between DNAm and PRC2 in regulation of this locus. To explore this relationship further, we examined expression of Dnmts in *Ezh2*<sup>-/-</sup> and wild-type mESCs. We found that expression of the *de novo* DNA methyltransferases, particularly Dnmt3a and Dnmt3l, were up-regulated in *Ezh2*<sup>-/-</sup> mESCs (Figures 4A–4B). Expression of Dnmt1, which is responsible for DNAm maintenance, was not significantly altered in *Ezh2*<sup>-/-</sup> mESCs (Figures 4A–4B). Additionally, we observed up-regulation of Dnmt3a and Dnmt3l in *Eed*<sup>-/-</sup> and *Jarid2*<sup>-/-</sup> mESCs (Figure S4A). *Ezh2* expression was unaffected in absence of any Dnmts (Figure S4B). Co-immunoprecipitation revealed that *Ezh2*, as well as *Jarid2*, interacts with Dnmt3a/Dnmt3l proteins (Figure 4C and Figures S4C, S4E). Moreover, Dnmt3a and Dnmt3l were both eluted in the same fractions as PRC2 components (*Ezh2*, *Jarid2* and *Suz12*) (Figure S4D), consistent with interaction between PRC2 and Dnmt3a/3l. We asked whether interaction between *Ezh2* and Dnmt3a/3l is dependent on *Gtl2* lncRNA. To test this, we used biallelic IG-DMR<sup>-/-</sup> mESCs, in which expression of maternal *Gtl2* lncRNA is abrogated (Figures 3F & 4D). Interaction between *Ezh2* and Dnmt3a/Dnmt3l was observed in the absence of *Gtl2* lncRNA (Figure 4D). Nonetheless, *Gtl2* lncRNA binds to PRC2 components (*Ezh2*, *Eed* and *Suz12*), but not detectably to Dnmt3a (Figures 4E & S4F). Thus, the interaction between PRC2 and Dnmt3a/3l is *Gtl2* lncRNA-independent. Of note, interactions between *Gtl2* lncRNA and PRC2 components (*Ezh2*, *Eed* and *Suz12*) (Figure S4F), as well as interactions between PRC2 components (Figure S4E), suggest that assembly or interactions of PRC2 complex components are not prevented in presence of *Gtl2* lncRNA.

PRC2 transcriptome analysis identified a genome-wide pool of >9000 PRC2-interacting RNAs, including *Gtl2* lncRNA, in mESCs (Zhao et al., 2010). The majority of these PRC2-interacting RNAs recruit PRC2 itself at their targets for gene repression (Margueron and Reinberg, 2011). However, recent studies demonstrated that *Ezh2*/PRC2 is located at a large fraction of “active promoters”, where it binds to the nascent RNAs that somehow reduce deposition of H3K27me3 (Davidovich et al., 2013; Kaneko et al., 2013). Interestingly, these active promoters reveal low-level occupancy by *Ezh2* (Kaneko et al., 2013). Further studies showed that deletion of PRC2-interacting RNA/s rescued PRC2-mediated deposition of H3K27me3 (Kaneko et al., 2014), implying that PRC2 activity is inhibited by interaction with nascent transcripts. We hypothesized that similarly binding of nascent *Gtl2* lncRNA to *Ezh2* (Figure 4E) inhibits interaction of *Ezh2*/PRC2 at the IG-DMR and subsequent deposition of H3K27me3. To support this, we showed that *Gtl2* promoter deletion disrupts the formation of *Gtl2* lncRNA, and is associated with increased binding of *Ezh2* at the IG-DMR locus (Figures 4F–4G). We did not observe, however, a significant increase in H3K27me3 at the IG-DMR (Figure 4H).

### PRC2 antagonizes *de novo* DNAm at the IG-DMR through a distinct mechanism

Next, we determined the occupancy of Dnmt3a, Dnmt3b, Dnmt3l and Dnmt1 at the IG-DMR locus in the absence of PRC2. Occupancy of Dnmt3a, Dnmt3b and Dnmt3l was markedly increased at the IG-DMR locus in the absence of Ezh2 or Jarid2 (Figures 5A–5B). We note that recruitment of Dnmt3a/3b/3l is higher at the IG-DMR in the absence of Ezh2 as compared to the absence of Jarid2, which may indicate that components of PRC2 have different capacities to modulate *de novo* Dnmt3s occupancy/ recruitment at the IG-DMR. We pursued this observation further by examining DNAm levels at the IG-DMR in *Ezh2*<sup>-/-</sup>, *Eed*<sup>-/-</sup> and *Jarid2*<sup>-/-</sup> mESCs. Indeed, different extents of DNA hypermethylation were observed at the IG-DMR in the absence of the distinct PRC2 components (Figure 5C). Importantly, DNA hypermethylation levels at the IG-DMR correlated with reduced expression levels of maternal lncRNAs and miRNAs at the *Gtl2-Rian-Mirg* locus in absence of Ezh2, Eed and Jarid2 (Figures 1 and S1). In summary, these data suggest that PRC2 prevents recruitment of Dnmt3s for *de novo* DNAm at the IG-DMR to allow proper expression of the maternal *Gtl2-Rian-Mirg* locus.

To exclude the trivial possibility that increased binding of Dnmt3 methyltransferases and DNAm at the IG-DMR is due to increased levels of *de novo* Dnmt3 methyltransferases in the absence of Ezh2, we performed global DNA methylation (DNAm) analysis from *Ezh2*<sup>-/-</sup> and wild-type mESCs, using reduced-representation bisulfite sequencing (RRBS). We observed gain of DNAm globally in the absence of Ezh2 (Figure 5D). Particularly, DNAm is gained at Ezh2 binding sites, in the absence of Ezh2 (Figure S5G). These data indicate the Ezh2 antagonizes Dnmt3 methyltransferases activity and DNAm in mESCs.

To investigate whether this mechanism is restricted to the maternal *Gtl2-Rian-Mirg* imprinted locus, we examined histone marks, PRC2 occupancy, and DNAm at several differentially regulated imprinted loci, including *H19*, whose expression is also significantly reduced in absence of PRC2 (Figure S1K). Occupancy of H3K27ac and H3K4me3 was significantly reduced at both the imprinting control regions- IG-DMR (for *Gtl2-Rian-Mirg* locus) and ICR (for *H19*) in the absence of Ezh2, correlating with reduced expression of Gtl2, Rian and H19. Interestingly, the ICR of *H19* is strongly occupied by Ezh2/PRC2 with corresponding H3K27me3 deposition, and acquires DNAm in the absence of Ezh2/PRC2, whereas the IG-DMR is weakly occupied by Ezh2/PRC2 without H3K27me3, yet gains DNAm in the absence of Ezh2/PRC2 (Figures S5A–S5F). These findings are consistent with antagonism between PRC2 and DNAm at both loci, but hint at differences in detail in mechanism.

### PRC2 protects IG-DMR from *de novo* DNAm to allow proper expression of the maternal *Gtl2-Rian-Mirg* locus

We demonstrated that Gtl2 lncRNA inhibits strong Ezh2/PRC2 occupancy and subsequent H3K27me3 deposition at the IG-DMR locus (Figure 3 and Figures 4F–4H). Therefore, we proposed that Ezh2 occupancy is weak at the IG-DMR, and it may be present in the vicinity of the locus in association with Gtl2 lncRNA. To address the mechanistic details of how Ezh2 prevents Dnmt3s occupancy/ recruitment and DNAm at the IG-DMR locus, first we performed a time course experiment after knockdown of Ezh2. Knockdown of Ezh2 showed



reduced expression of Gtl2 lncRNA and increased expression of Dnmt3a (Figures S6A–S6B), similar to, but quantitatively less extreme than the pattern observed upon complete deletion of Ezh2 (Figures 1D & 4B; Figures S6A–S6B). However, knockdown of Ezh2 did not increase the DNAm level at the IG-DMR, as we observed in *Ezh2*<sup>-/-</sup> mESCs (Figures S6C & 2C). On the other hand, deletion of *Dnmt3a* (*Dnmt3a*<sup>-/-</sup>) showed a modest increase in Gtl2 expression, but no significant change in DNAm at the IG-DMR (Figures S6D–S6E). In addition, depletion of Ezh2 in *Dnmt3a*<sup>-/-</sup> mESCs reduced Gtl2 expression (Figure S6F), indicating a positive function of Ezh2/PRC2 at the maternal *Gtl2-Rian-Mirg* locus.

Furthermore, we overexpressed Ezh2 and Dnmt3a in wild-type mESCs. Overexpression of neither Ezh2 nor Dnmt3a altered Gtl2 expression and DNAm at the IG-DMR (Figures 6A–6F). In addition, overexpression of Ezh2 in *Dnmt3a*<sup>-/-</sup> mESCs showed no significant change in Gtl2 expression and DNAm at the IG-DMR (Figures 6G–6I), implying that Ezh2 does not function as an activator at the IG-DMR locus. Taken together, these data support that Ezh2 functions to “protect” the IG-DMR locus from Dnmt3s/DNAm and thereby serves to maintain expression of the maternal *Gtl2-Rian-Mirg* locus.

## DISCUSSION

The precise mechanisms regulating imprinting at the *Dlk1-Dio3* domain have remained largely unknown (Rocha et al., 2008). Here, we demonstrate that PRC2 is required for proper expression of the maternal *Gtl2-Rian-Mirg* locus, a cluster essential for successful iPSC reprogramming (Figure S7A) (Stadtfield et al., 2010). Absence of PRC2 results in markedly elevated DNAm at the IG-DMR leading to transcriptional repression of the entire maternal *Gtl2-Rian-Mirg* locus (Figures 1 and 2). The maternal IG-DMR is lowly methylated/ hypomethylated and acts as an “enhancer” of the maternal *Gtl2-Rian-Mirg* locus due to co-occupancy of ESC-specific TFs, mediators, cohesin, Lsd1, H3K27ac and H3K4me1 (Figure 3). This finding is consistent with the observation that lowly methylated regions (LMRs) serve as distal regulatory regions and act as enhancers (Stadler et al., 2011).

Since Gtl2 lncRNA binds to Ezh2, the occupancy of Ezh2 is weak and H3K27me3 deposition does not take place at the IG-DMR of maternal *Gtl2-Rian-Mirg* locus (Figures 3A, 3C, 4E–4H). Nonetheless, we propose that the presence of Ezh2/PRC2 protects the IG-DMR locus from recruitment of Dnmt3s and subsequent DNAm. Several lines of evidence support this model. First, Ezh2 and Dnmt3a/3l physically interact (Figure 4C). Second, Dnmt3s binding to the IG-DMR is increased (Figures 5A–5B) and DNA is strongly methylated in the absence of Ezh2 (and PRC2). (Figures 2C & 5C). Third, DNA methylation is globally increased at Ezh2 binding sites in the absence of Ezh2 (Figure 5D). Finally, neither overexpression of Ezh2 or Dnmt3a in wild-type ESCs, nor overexpression of Ezh2 in *Dnmt3a*<sup>-/-</sup> ESCs, alters DNA methylation at the IG-DMR and Gtl2 lncRNA expression (Figure 6). In effect, Ezh2/PRC2 then protects the IG-DMR locus from Dnmt3s and its activity (i.e. DNAmethylation).

Generally the presence of Ezh2/PRC2 correlates with gene repression (Margueron and Reinberg, 2011). However, two recent reports demonstrate that PRC2 localizes not only at the promoter regions of repressed genes, but also at the promoters of the active genes.

Remarkably, PRC2 weakly occupies active promoter regions (with reduced level of H3K27me3) and binds to the 5' terminus of nascent transcripts, which originate from active genes (Davidovich et al., 2013; Kaneko et al., 2013). These results suggest that PRC2 senses the transcription activity of genes through nascent RNA binding that tempers Ezh2/PRC2 activity (Kaneko et al., 2013). This scenario may allow continuous expression of active genes by cell-type specific TFs, activators, despite the presence of PRC2. A similar phenomenon may drive continuous expression of the maternal *Gtl2-Rian-Mirg* locus in association with ESC-specific TFs, mediators, cohesin, H3K27ac and H3K4me1 at the IG-DMR despite the presence of Ezh2/PRC2 in association with Gtl2 lncRNA (Figure 7).

Our findings focus attention on the relationship of polycomb function and DNA methylation. Both pathways are involved in the establishment and maintenance of epigenetic gene silencing. Some evidence points to a cooperative relationship between DNAm and PRC2, where PRC2 facilitates binding (or recruitment) of DNA methyltransferases (Dnmt) at PRC2 target promoters to promote DNA methylation (Viré et al., 2005). This scenario has been proposed in colon cancer, where Ezh2/PRC2 has been reported to recruit DNA methyltransferases for *de novo* DNAm to silence genes that are critical for normal colonic epithelium development (Schlesinger et al., 2006). Additionally, reduced levels of H3K27me3 and DNA hypomethylation concurrently activate gene expression in pediatric gliomas (Bender et al., 2013), implying that PRC2-mediated *de novo* DNAm contributes to carcinogenesis. In contrast, other evidence supports antagonism between DNAm and polycomb function. For example, genome-wide studies in mESCs reveal gain of H3K27me3 and DNAm upon loss of Dnmt methyltransferases and PRC2, respectively (Brinkman et al., 2012; Hagarman et al., 2013). Furthermore, developmentally related genes containing CpG islands that are silenced by PRC2 in normal cells acquire DNA methylation with loss of PRC2 marks in prostate cancer (Gal-Yam et al., 2008). Also, loss of Dnmt3a leads to an increased level of H3K27me3 in neural stem cells (Wu et al., 2010). Of particular note, a recent study implicates PRC2 in direct regulation of Dnmt3l (Basu et al., 2014), which is consistent with our observation of increased expression of Dnmt3s upon loss of Ezh2/PRC2 (Figures 4A–4B). In addition, links between DNA hypomethylation and accumulation and/or spreading of H3K27me3 have been proposed in cancer (Reddington et al., 2013). Thus, the relationship between DNAm and PRC2 may be critical in both normal and cancer cells. Our data provide additional insights into the relationship between PRC2 and DNA methyltransferases. PRC2 interacts physically with Dnmt3a/3l in a *Gtl2* lncRNA-independent manner and prevents Dnmt3s recruitment and subsequent DNAm at the IG-DMR of maternal *Gtl2-Rian-Mirg* locus (Figures 4, 5 and 6). Dnmt3a/3l forms a tetramer for *de novo* DNAm (Jia et al., 2007). Dnmt3l shares homology with Dnmt3a and Dnmt3b, but lacks enzymatic activity, although Dnmt3l cooperates with Dnmt3a and Dnmt3b to establish maternal imprinting (Hata et al., 2002). Furthermore, Dnmt3l has been shown to enhance the *de novo* DNAm activity of Dnmt3a (Chedin et al., 2002), which implicates Dnmt3l as an important cofactor for Dnmt3a. In addition, conditional mutants of *Dnmt3a* and *Dnmt3l* in germs cells display indistinguishable phenotypes; however, conditional mutants of *Dnmt3b* demonstrate no apparent phenotype indicating that Dnmt3a and Dnmt3l function together for DNAm at many of the imprinted loci in germ cells (Kaneda et al., 2004).

Although our findings are consistent with a model in which Ezh2 protects the IG-DMR locus from Dnmt3s recruitment and subsequent DNAm to maintain proper expression of the maternal *Gtl2-Rian-Mirg* locus, further study is needed to address more specific mechanisms issues. For one, it remains to be determined how and to what extent other PRC2 components, such as Eed, Suz12, and Jarid2 are involved in protecting the IG-DMR from DNAm. Second, the mechanism by which Gtl2 lncRNA inhibits binding of Ezh2/PRC2 at the IG-DMR and contributes to decreased H3K27me3 activity merits further clarification. Moreover, precisely how Gtl2 lncRNA recruits Ezh2/PRC2 at the IG-DMR and maintains its own expression through a feedback loop is not fully explored.

In conclusion, we demonstrated that Gtl2 lncRNA inhibits binding of Ezh2/PRC2 at the maternal IG-DMR locus, while Ezh2/PRC2 maintains its presence in the vicinity of the IG-DMR locus. In this manner, Ezh2/PRC2 protects the maternal IG-DMR locus by preventing recruitment of Dnmt3s and subsequent DNAm, thereby serving to maintain expression of the maternal *Gtl2-Rian-Mirg* locus in the presence of ESC-specific TFs and activators (Figure 7). In the absence of Ezh2, Dnmt3s is then recruited to and methylates the IG-DMR, leading to transcription repression of the maternal *Gtl2-Rian-Mirg* locus (Figure 7). Our findings also suggest that individual PRC2 components have different capacities to modulate Dnmt3s occupancy/recruitment and subsequent *de novo* DNAm at the IG-DMR (Figure 5), which ultimately sets different levels of expression of maternal lncRNAs and miRNAs from *Gtl2-Rian-Mirg* locus (Figure 1). Collectively, our study provides a novel mechanism by which Ezh2/PRC2 antagonizes *de novo* DNA methylation at the IG-DMR for proper expression of maternal *Gtl2-Rian-Mirg* locus, a critical region essential for mESCs identity and somatic cell reprogramming (Pereira et al., 2010; Stadtfeld et al., 2010).

## EXPERIMENTAL PROCEDURES

### Mouse ES cell culture

Mouse CJ7 (wild-type), *Ezh2*<sup>-/-</sup>, *Eed*<sup>-/-</sup>, *Jarid2*<sup>-/-</sup> and other mES cell lines were maintained in ES medium: DMEM (Dulbecco's modified Eagle's medium-Life Technologies) supplemented with 15% fetal calf serum (Life Technologies), 0.1 mM  $\beta$ -mercaptoethanol (Sigma), 2 mM L-glutamine (Life Technologies), 0.1 mM nonessential amino acid (Life Technologies), 1% of nucleoside mix (Sigma), 1000 U/ml recombinant leukemia inhibitory factor (LIF; Chemicon), and 50 U/ml penicillin/streptomycin (Life Technologies). *Ezh2*<sup>-/-</sup>, *Eed*<sup>-/-</sup> and *Jarid2*<sup>-/-</sup> mESCs were established previously (Shen et al., 2008; Shen et al., 2009; Xie et al., 2014).

### Small RNA sequencing (RNA-Seq)

Total RNA was isolated from undifferentiated mESCs using Trizol reagent (Invitrogen) according to the manufacturer's instructions. 10  $\mu$ g of total RNA from CJ7 (wild-type), *Ezh2*<sup>-/-</sup>, *Eed*<sup>-/-</sup>, and *Jarid2*<sup>-/-</sup> mESCs were size selected to 18–40 nucleotides on a denaturing polyacrylamide gel and small RNA libraries were prepared according to manufacturer's instructions (SOLiD small RNA library preparation kit, Life Technologies). All libraries were sequenced using SOLiD instrument (Life Technologies).

### **RNA sequencing (RNA-Seq)**

Total RNA was isolated from undifferentiated mESCs using Trizol reagent (Invitrogen) according to the manufacturer's instructions. 1µg of total RNA was used from CJ7 (wild-type), *Ezh2*<sup>-/-</sup>, *Eed*<sup>-/-</sup>, and *Jarid2*<sup>-/-</sup> mESCs to prepare the mRNA libraries according to the manufacturer's instructions (Directional (strand specific) mRNA-Seq sample preparation kit, Illumina). All libraries were sequenced using HiSeq 2000 sequencing system (Illumina).

### **Northern blot**

10µg of total RNA was resolved in denaturing PAGE, transferred to a nitrocellulose membrane and hybridized with DNA or LNA probes specific to each miRNA as described before (Das et al., 2008).

### **Quantitative RT-PCR**

Total RNA was isolated from mESCs using RNeasy plus kit (Qiagen) or Trizol (Invitrogen), and treated with DNaseI (Life Technologies) to remove the DNA contamination. RNA was converted to cDNA with a cDNA synthesis kit (Bio-Rad). qRT-PCR was performed with SYBR green master mix (Bio-Rad) on Bio-Rad iCycler RT-PCR detection system according to manufacture's instructions. Small RNA RT-PCR was performed using Taqman miRNA assays (Life Technologies) as described before (Das et al., 2008) .

### **ChIP**

ChIP were performed as described elsewhere (Das et al., 2014). Detailed procedures and a list of antibodies are available in supplemental information.

### **ChIP sequencing (ChIP-Seq) and Library Generation**

Purified ChIP DNA was used to prepare Illumina multiplexed sequencing libraries. NEB next generation sequencing kit was used to prepare the libraries.

### **ChIP-Seq data analyses**

All ChIP-Seq samples were aligned with Bowtie v0.12.9 to the mm9 genome assembly, where only uniquely mappable reads were reported. Significant peaks were found by pairing each ChIP-Seq sample with the appropriate input, and running SICER v1.1, with a false discovery rate (FDR) of 0.05. See the supplementary information section for more detail.

### **DNA methylation analysis**

Genomic DNA was bisulphate converted and analyzed by EpigenDx using following assays: IG-DMR (ADS-1452), Oct4 promoter (ASY-585) and Nanog promoter (ASY-590).

### **Supplementary Material**

Refer to Web version on PubMed Central for supplementary material.

## Acknowledgments

We thank Pratibha Tripathi, Glenn MacLean for reagents, Fieda Abderazzaq and Renee Rubio at the CCCB sequencing facility, Dana Farber Cancer Institute (DFCI) for Illumina HiSeq2000 Sequencing, and the late Edward Fox at the Microarray Core of DFCI for microarray and small RNA sequencing. This work was supported by funding from NIH Grant HLBI U01HL100001. S.H.O. is an Investigator of the Howard Hughes Medical Institute (HHMI). The authors declare no competing financial interests.

## References

- Basu A, Dasari V, Mishra RK, Khosla S. The CpG Island Encompassing the Promoter and First Exon of Human DNMT3L Gene Is a PcG/TrX Response Element (PRE). *PLoS ONE*. 2014; 9:e93561. [PubMed: 24743422]
- Bender S, Tang Y, Lindroth AM, Hovestadt V, Jones DTW, Kool M, Zapatka M, Northcott PA, Sturm D, Wang W, et al. Reduced H3K27me3 and DNA Hypomethylation Are Major Drivers of Gene Expression in K27M Mutant Pediatric High-Grade Gliomas. *Cancer Cell*. 2013; 24:660–672. [PubMed: 24183680]
- Bernstein BE, Mikkelsen TS, Xie X, Kamal M, Huebert DJ, Cuff J, Fry B, Meissner A, Wernig M, Plath K, et al. A Bivalent Chromatin Structure Marks Key Developmental Genes in Embryonic Stem Cells. *Cell*. 2006; 125:315–326. [PubMed: 16630819]
- Boyer LA, Plath K, Zeitlinger J, Brambrink T, Medeiros LA, Lee TI, Levine SS, Wernig M, Tajonar A, Ray MK, et al. Polycomb complexes repress developmental regulators in murine embryonic stem cells. *Nature*. 2006; 441:349–353. [PubMed: 16625203]
- Brinkman AB, Gu H, Bartels SJJ, Zhang Y, Matarese F, Simmer F, Marks H, Bock C, Gnirke A, Meissner A, et al. Sequential ChIP-bisulfite sequencing enables direct genome-scale investigation of chromatin and DNA methylation cross-talk. *Genome Research*. 2012; 22:1128–1138. [PubMed: 22466170]
- Brookes E, de Santiago I, Hebenstreit D, Morris KJ, Carroll T, Xie SQ, Stock JK, Heidemann M, Eick D, Nozaki N, et al. Polycomb Associates Genome-wide with a Specific RNA Polymerase II Variant, and Regulates Metabolic Genes in ESCs. *Cell Stem Cell*. 2012; 10:157–170. [PubMed: 22305566]
- Chedin F, Lieber MR, Hsieh C-L. The DNA methyltransferase-like protein DNMT3L stimulates de novo methylation by Dnmt3a. *PNAS*. 2002; 99(26):16916–21. [PubMed: 12481029]
- Cong L, Ran FA, Cox D, Lin S, Barretto R, Habib N, Hsu PD, Wu X, Jiang W, Marraffini LA, et al. Multiplex Genome Engineering Using CRISPR/Cas Systems. *Science*. 2013; 339:819–823. [PubMed: 23287718]
- Das PP, Bagijn MP, Goldstein LD, Woolford JR, Lehrbach NJ, Sapetschnig A, Buhecha HR, Gilchrist MJ, Howe KL, Stark R, et al. Piwi and piRNAs Act Upstream of an Endogenous siRNA Pathway to Suppress Tc3 Transposon Mobility in the *Caenorhabditis elegans* Germline. *Molecular Cell*. 2008; 31:79–90. [PubMed: 18571451]
- Das PP, Shao Z, Beyaz S, Apostolou E, Pinello L, De Los Angeles A, O'Brien K, Atsma JM, Fujiwara Y, Nguyen M, et al. Distinct and Combinatorial Functions of Jmjd2b/Kdm4b and Jmjd2c/Kdm4c in Mouse Embryonic Stem Cell Identity. *Molecular Cell*. 2014; 53:32–48. [PubMed: 24361252]
- Davidovich C, Zheng L, Goodrich KJ, Cech TR. Promiscuous RNA binding by Polycomb repressive complex 2. *Nature Structural Molecular Biology*. 2013; 20:1250–1257.
- Dong KB, Maksakova IA, Mohn F, Leung D, Appanah R, Lee S, Yang HW, Lam LL, Mager DL, Schubeler D, Tachibana M, Shinkai Y, Lorincz MC. DNA methylation in ES cells requires the lysine methyltransferase G9a but not its catalytic activity. *EMBO*. 2008:1–11.
- Edwards CA, Ferguson-Smith AC. Mechanisms regulating imprinted genes in clusters. *Current Opinion in Cell Biology*. 2007; 19:281–289. [PubMed: 17467259]
- Epsztejn-Litman S, Feldman N, Abu-Remaileh M, Shufaro Y, Gerson A, Ueda J, Deplus R, Fuks F, Shinkai Y, Cedar H, et al. De novo DNA methylation promoted by G9a prevents reprogramming of embryonically silenced genes. *Nature Publishing Group*. 2008; 15:1176–1183.
- Ferrari KJ, Scelfo A, Jammula S, Cuomo A, Barozzi I, Stützer A, Fischle W, Bonaldi T, Pasini D. Polycomb-Dependent H3K27me1 and H3K27me2 Regulate Active Transcription and Enhancer Fidelity. *Molecular Cell*. 2014; 53:49–62. [PubMed: 24289921]



- Gal-Yam EN, Egger G, Iniguez L, Holster H, Einarsson S, Zhang X, Lin JC, Liang G, Jones PA, Tanay A. Frequent switching of Polycomb repressive marks and DNA hypermethylation in the PC3 prostate cancer cell line. *PNAS*. 2008; 105:12979–84. [PubMed: 18753622]
- Hagarman JA, Motley MP, Kristjansdottir K, Soloway PD. Coordinate Regulation of DNA Methylation and H3K27me3 in Mouse Embryonic Stem Cells. *PLoS ONE*. 2013; 8:e53880. [PubMed: 23326524]
- Hata K, Okano M, Lei H, Li E. Dnmt3L cooperates with the Dnmt3 family of de novo DNA methyltransferases to establish maternal imprints in mice. *Development*. 2002; 129:1983–1993. [PubMed: 11934864]
- Jia D, Jurkowska RZ, Zhang X, Jeltsch A, Cheng X. Structure of Dnmt3a bound to Dnmt3L suggests a model for de novo DNA methylation. *Nature*. 2007; 449:248–251. [PubMed: 17713477]
- Kagey MH, Newman JJ, Bilodeau S, Zhan Y, Orlando DA, van Berkum NL, Ebmeier CC, Goossens J, Rahl PB, Levine SS, et al. Mediator and cohesin connect gene expression and chromatin architecture. *Nature*. 2010; 467:430–435. [PubMed: 20720539]
- Kaneda M, Okano M, Hata K, Sado T, Tsujimoto N, Li E, Sasaki H. Essential role for de novo DNA methyltransferase Dnmt3a in paternal and maternal imprinting. *Nature*. 2004; 429:900–903. [PubMed: 15215868]
- Kaneko S, Son J, Shen SS, Reinberg D, Bonasio R. PRC2 binds active promoters and contacts nascent RNAs in embryonic stem cells. *Nature Structural Molecular Biology*. 2013; 20:1258–1264.
- Kaneko S, Son J, Bonasio R, Shen SS, Reinberg D. Nascent RNA interaction keeps PRC2 activity poised and in check. *Genes & Development*. 2014; 28:1983–1988. [PubMed: 25170018]
- Kanhere A, Viiri K, Araújo CC, Rasaiyaah J, Bouwman RD, Whyte WA, Pereira CF, Brookes E, Walker K, Bell GW, et al. Short RNAs Are Transcribed from Repressed Polycomb Target Genes and Interact with Polycomb Repressive Complex-2. *Molecular Cell*. 2010; 38:675–688. [PubMed: 20542000]
- Ku M, Koche RP, Rheinbay E, Mendenhall EM, Endoh M, Mikkelsen TS, Presser A, Nusbaum C, Xie X, Chi AS, et al. Genome wide Analysis of PRC1 and PRC2 Occupancy Identifies Two Classes of Bivalent Domains. *PLoS Genet*. 2008; 4:e1000242. [PubMed: 18974828]
- Lin SP, Youngson N, Takada S, Seitz H, Reik W, Paulsen M, Cavaille J, Ferguson-Smith AC. Asymmetric regulation of imprinting on the maternal and paternal chromosomes at the Dlk1-Gtl2 imprinted cluster on mouse chromosome 12. *Nature Genetics*. 2003; 35:97–102. [PubMed: 12937418]
- Margueron R, Reinberg D. The Polycomb complex PRC2 and its mark in life. *Nature*. 2011; 469:343–349. [PubMed: 21248841]
- Mikkelsen TS, Ku M, Jaffe DB, Issac B, Lieberman E, Giannoukos G, Alvarez P, Brockman W, Kim TK, Koche RP, et al. Genome-wide maps of chromatin state in pluripotent and lineage-committed cells. *Nature*. 2007; 448:553–560. [PubMed: 17603471]
- Pandey RR, Mondal T, Mohammad F, Enroth S, Redrup L, Komorowski J, Nagano T, Mancini-DiNardo D, Kanduri C. Kcnq1ot1 Antisense Noncoding RNA Mediates Lineage-Specific Transcriptional Silencing through Chromatin-Level Regulation. *Molecular Cell*. 2008; 32:232–246. [PubMed: 18951091]
- Pereira CF, Piccolo FM, Tsubouchi T, Sauer S, Ryan NK, Bruno L, Landeira D, Santos J, Banito A, Gil J, et al. ESCs Require PRC2 to Direct the Successful Reprogramming of Differentiated Cells toward Pluripotency. *Cell Stem Cell*. 2010; 6:547–556. [PubMed: 20569692]
- Reddington JP, Sproul D, Meehan RR. DNA methylation reprogramming in cancer: Does it act by reconfiguring the binding landscape of Polycomb repressive complexes? *Bio Essays*. 2013; 36:134–140.
- Rinn JL, Kertesz M, Wang JK, Squazzo SL, Xu X, Bruggmann SA, Goodnough LH, Helms JA, Farnham PJ, Segal E, et al. Functional Demarcation of Active and Silent Chromatin Domains in Human HOX Loci by Noncoding RNAs. *Cell*. 2007; 129:1311–1323. [PubMed: 17604720]
- Rocha STD, Edwards CA, Ito M, Ogata T, Ferguson-Smith AC. Genomic imprinting at the mammalian Dlk1-Dio3 domain. *Trends in Genetics*. 2008; 24:306–316. [PubMed: 18471925]
- Schlesinger Y, Straussman R, Keshet I, Farkash S, Hecht M, Zimmerman J, Eden E, Yakhini Z, Ben-Shushan E, Reubinoff BE, et al. Polycomb-mediated methylation on Lys27 of histone H3 pre-

- marks genes for de novo methylation in cancer. *Nature Genetics*. 2006; 39:232–236. [PubMed: 17200670]
- Shen X, Liu Y, Hsu YJ, Fujiwara Y, Kim J, Mao X, Yuan GC, Orkin SH. EZH1 Mediates Methylation on Histone H3 Lysine 27 and Complements EZH2 in Maintaining Stem Cell Identity and Executing Pluripotency. *Molecular Cell*. 2008; 32:491–502. [PubMed: 19026780]
- Shen X, Kim W, Fujiwara Y, Simon MD, Liu Y, Mysliwiec MR, Yuan GC, Lee Y, Orkin SH. Jumonji Modulates Polycomb Activity and Self-Renewal versus Differentiation of Stem Cells. *Cell*. 2009; 139:1303–1314. [PubMed: 20064376]
- Simon JA, Kingston RE. Mechanisms of Polycomb gene silencing: knowns and unknowns. *Nature Reviews Molecular Cell Biology*. 2009:1–12.
- Smith ZD, Meissner A. DNA methylation: roles in mammalian development. *Nature Reviews Genetics*. 2013; 14:204–220.
- Stadler MB, Murr R, Burger L, Ivanek R, Lienert F, Schöler A, van Nimwegen E, Wirbelauer C, Oakeley EJ, Gaidatzis D, et al. DNA-binding factors shape the mouse methylome at distal regulatory regions. *Nature*. 2011:1–7.
- Stadtfield M, Apostolou E, Akutsu H, Fukuda A, Follett P, Natesan S, Kono T, Shioda T, Hochedlinger K. Aberrant silencing of imprinted genes on chromosome 12qF1 in mouse induced pluripotent stem cells. *Nature*. 2010; 465:175–181. [PubMed: 20418860]
- Stadtfield M, Apostolou E, Ferrari F, Choi J, Walsh RM, Chen T, Ooi SSK, Kim SY, Bestor TH, Shioda T, et al. Ascorbic acid prevents loss of Dlk1-Dio3 imprinting and facilitates generation of all-iPS cell mice from terminally differentiated B cells. *Nature Genetics*. 2012; 44:398–405. [PubMed: 22387999]
- Takahashi K, Yamanaka S. Induction of Pluripotent Stem Cells from Mouse Embryonic and Adult Fibroblast Cultures by Defined Factors. *Cell*. 2006; 126:663–676. [PubMed: 16904174]
- Viré E, Brenner C, Deplus R, Blanchon L, Fraga M, Didelot C, Morey L, Van Eynde A, Bernard D, Vanderwinden JM, et al. The Polycomb group protein EZH2 directly controls DNA methylation. *Nature*. 2005; 439:871–874. [PubMed: 16357870]
- Whyte WA, Bilodeau S, Orlando DA, Hoke HA, Frampton GM, Foster CT, Cowley SM, Young RA. Enhancer decommissioning by LSD1 during embryonic stem cell differentiation. *Nature*. 2012; 482:221–225. [PubMed: 22297846]
- Wu H, Coskun V, Tao J, Xie W, Ge W, Yoshikawa K, Li E, Zhang Y, Sun YE. Dnmt3a-Dependent Nonpromoter DNA Methylation Facilitates Transcription of Neurogenic Genes. *Science*. 2010; 329:444–448. [PubMed: 20651149]
- Xie H, Xu J, Hsu JH, Nguyen M, Fujiwara Y, Peng C, Orkin SH. Polycomb Repressive Complex 2 Regulates Normal Hematopoietic Stem Cell Function in a Developmental-Stage-Specific Manner. *Cell Stem Cell*. 2014; 14:68–80. [PubMed: 24239285]
- Xie W, Barr CL, Kim A, Yue F, Lee AY, Eubanks J, Dempster EL, Ren B. Base-Resolution Analyses of Sequence and Parent-of-Origin Dependent DNA Methylation in the Mouse Genome. *Cell*. 2012; 148:816–831. [PubMed: 22341451]
- Zhao J, Sun BK, Erwin JA, Song JJ, Lee JT. Polycomb Proteins Targeted by a Short Repeat RNA to the Mouse X Chromosome. *Science*. 2008; 322:750–756. [PubMed: 18974356]
- Zhao J, Ohsumi TK, Kung JT, Ogawa Y, Grau DJ, Sarma K, Song JJ, Kingston RE, Borowsky M, Lee JT. Genome-wide Identification of Polycomb-Associated RNAs by RIP-seq. *Molecular Cell*. 2010; 40:939–953. [PubMed: 21172659]
- Zhou VW, Goren A, Bernstein BE. Charting histone modifications and the functional organization of mammalian genomes. *Nature Reviews Genetics*. 2010; 12:7–18.

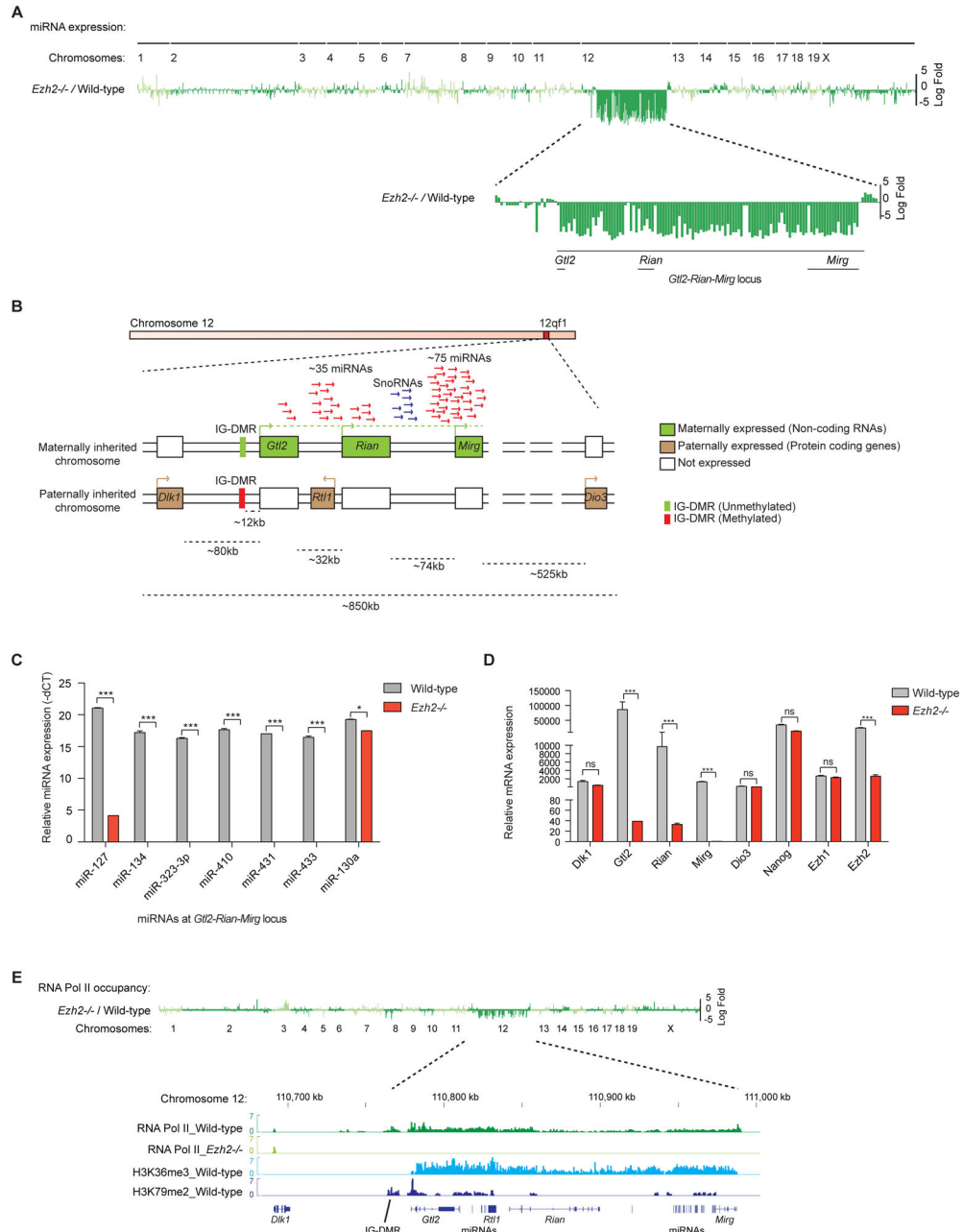


**Figure 1. PRC2 is required to maintain expression of maternal miRNAs and lncRNAs at the *Gtl2-Rian-Mirg* locus**

(A) Small RNA-seq demonstrates log-fold changes of miRNA expression in *Ezh2*<sup>-/-</sup> mESCs compared to wild-type. Significantly reduced expression of a cluster of miRNAs is observed at the *Gtl2-Rian-Mirg* locus of chromosome 12 in *Ezh2*<sup>-/-</sup> mESCs compared to wild-type.

(B) Schematic representation of the *Dlk1-Dio3* imprinted gene cluster. lncRNAs genes-*Gtl2*, *Rian* and *Mirg*, miRNAs and snoRNAs are expressed from “maternally” inherited chromosome, whereas, protein coding genes, *Dlk1*, *Dio3* and *Rtl1* are expressed from “paternally” inherited chromosome. Empty boxes represent genes that are repressed.

Imprinting is regulated by IG-DMR, which is methylated in paternally inherited chromosome, but unmethylated in maternally inherited chromosome. Therefore, by default all lncRNAs, miRNAs and snoRNAs from paternally inherited chromosome are repressed due to hypermethylation at IG-DMR, and only maternal ones are expressed.

(C) Quantitative RT-PCR (RT-qPCR) confirms dramatically reduced expression of maternal miRNAs from the *Gtl2-Rian-Mirg* locus in *Ezh2*<sup>-/-</sup> mESCs. miR-130a is shown as a control. miRNAs expression represented as mean  $\pm$  SEM (n=3); p-values were calculated using a 2-way ANOVA; \*\*\*p <0.0001, \*p <0.01.

(D) RT-qPCR shows dramatic reduction of maternal *Gtl2*, *Rian* and *Mirg* lncRNAs expression in *Ezh2*<sup>-/-</sup> mESCs as compared to wild-type. *Dlk1* and *Dio3* mRNA expressions are unaltered in *Ezh2*<sup>-/-</sup> mESCs. Transcript levels were normalized to *Gapdh*. Data are represented as mean  $\pm$  SEM (n=3); p-values were calculated using a 2-way ANOVA; \*\*\*p <0.0001, ns (non-significant).

(E) ChIP-seq analysis of RNA Pol II demonstrates log-fold changes of RNA Pol II occupancy in *Ezh2*<sup>-/-</sup> mESCs compared to wild-type. RNA Pol II occupancy is significantly reduced at the entire *Gtl2-Rian-Mirg* locus (~220kb) in *Ezh2*<sup>-/-</sup> mESCs compared to wild-type. RNA Pol II co-occupancy with H3K36me3 and H3K79me2 (elongation marks) suggests that the maternal *Gtl2-Rian-Mirg* locus acts as a single transcriptional unit.

See also Figure S1.

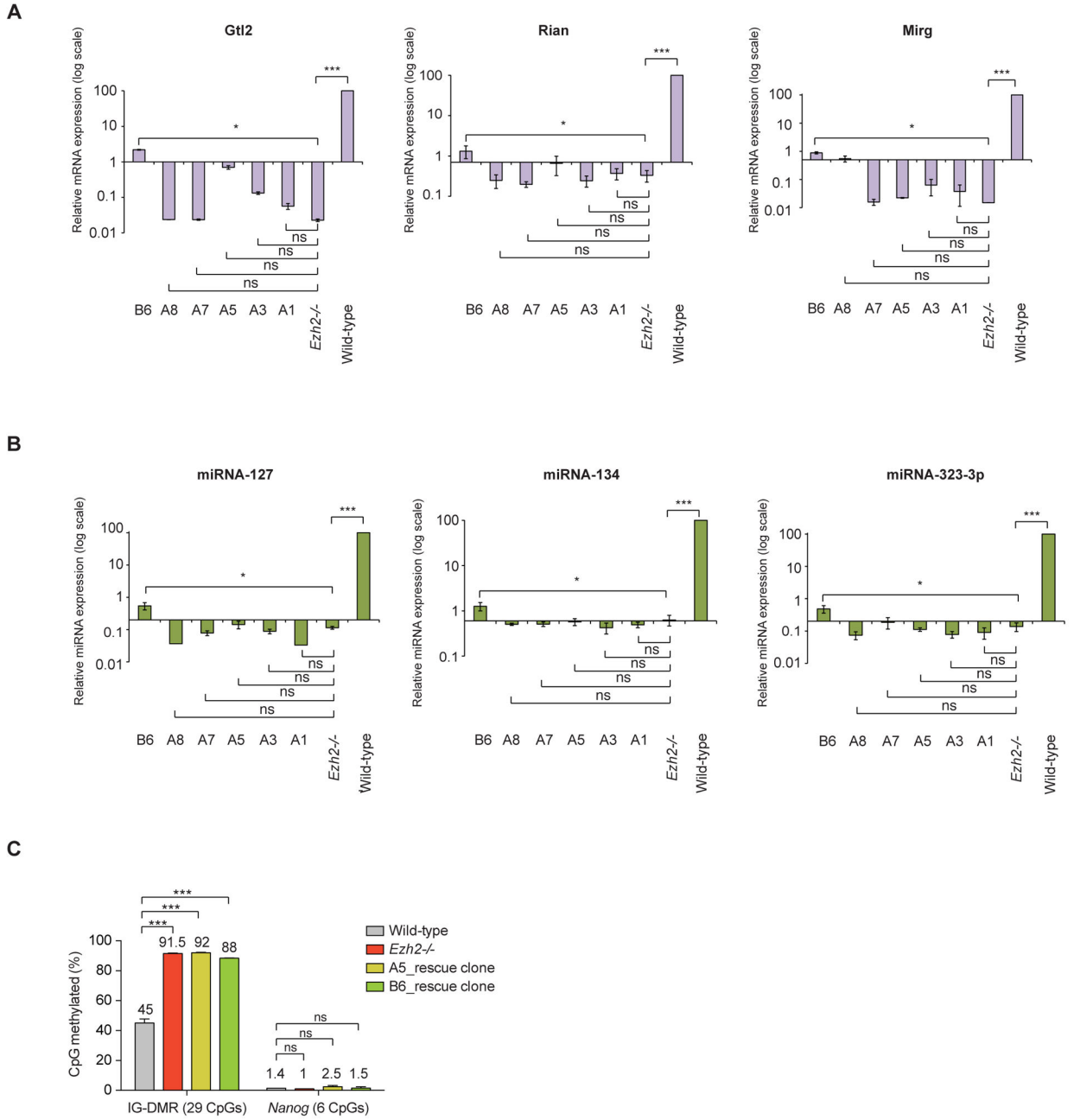


**Figure 2. Methylation of the *Gtl2-Rian-Mirg* locus in the absence of PRC2**

(A–B) Several independent *Ezh2* rescue clones express different levels of exogenous *Ezh2* (Figures S2A & S2C). Rescue clones with lower level of *Ezh2* expression fail to rescue the expression of maternal lncRNAs and miRNAs. *Ezh2* rescue clones, A5 and B6 that express at a near endogenous level of *Ezh2* (Figures S2A & S2C) also fail to restore the expression of maternal *Gtl2*, *Rian* and *Mirg* lncRNAs as well as miRNAs from the *Gtl2-Rian-Mirg* locus. mRNA transcript levels were normalized to *Gapdh*. Both mRNA and miRNA expressions are shown as mean  $\pm$  SEM (n=3); p-values were calculated using a one-way ANOVA; \*\*\*p < 0.0001, \*p < 0.01, ns (non-significant).



(C) Analysis of 29 CpGs at the IG-DMR shows gain of DNAm (%) in *Ezh2*<sup>-/-</sup> mESCs compared to wild-type. *Ezh2* rescue clones (A5 and B6) that expresses similar level of endogenous *Ezh2*, retains hypermethylation at IG-DMR, indicating stable establishment of DNAm at the IG-DMR in absence of *Ezh2*. DNAm at *Nanog* proximal promoter was used as a control. Data are represented as mean  $\pm$  SEM (n=3); p-values were calculated using a 2-way ANOVA; \*\*\*p < 0.0001, ns (non-significant).

See also Figure S2.

Author Manuscript

Author Manuscript

Author Manuscript

Author Manuscript

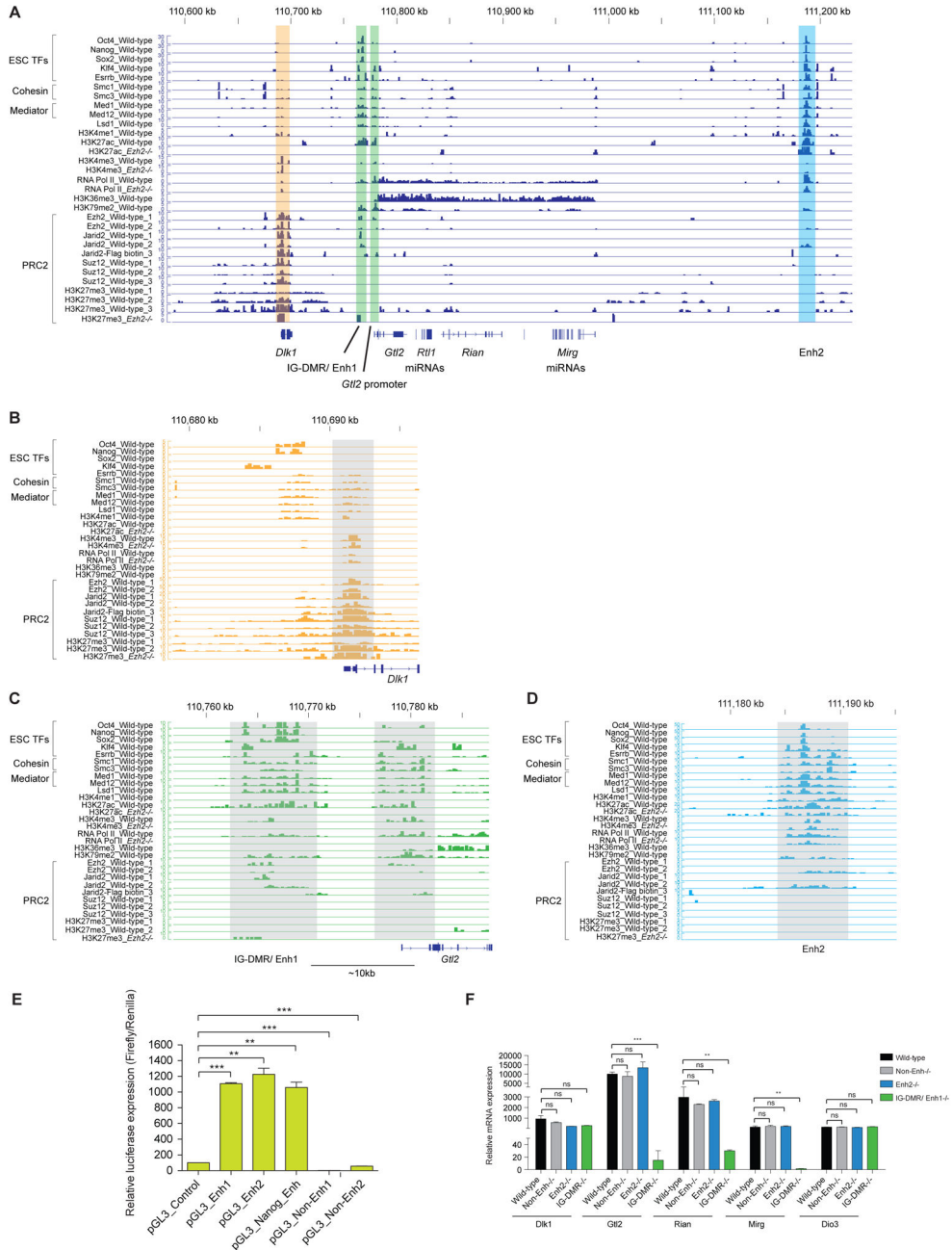


**Figure 3. IG-DMR/Enhancer1 serves as an enhancer for the *Gtl2-Rian-Mirg* locus**  
 (A–D) Co-occupancy of ESC-specific TFs (e.g. Oct4, Nanog, Sox2, Klf4, Esrrb), mediator (Med1/12), cohesin (Smc1/3), Lsd1, H3K27ac and H3K4me1 at IG-DMR/Enh1 and Enh2 fulfills criteria for putative enhancer regions of *Gtl2-Rian-Mirg* locus. The zoomed in shaded regions show *Dik1* promoter, IG-DMR/Enh1, *Gtl2* promoter and Enh2 regions, which are occupied with several factors and histones marks in *Ezh2*<sup>-/-</sup> and wild-type mESCs. Multiple individual Chip-seq genomic tracks of PRC2 components show weak occupancy of Ezh2, Jarid2 and no binding of Suz12 of PRC2 components at the IG-DMR/Enh1 and Enh2, and failed to observe detectable H3K27me3 deposition.

(E) Luciferase reporter assays of Enh1 and Enh2 demonstrate strong enhancer activity as *Nanog* enhancer. Non-Enh1 and Non-Enh2 (lacks binding of any of the factors and histone marks, see Figure. S3A) both were used as controls. Data are represented as mean  $\pm$  SEM (n=3); p-values were calculated using a 2-way ANOVA; \*\*\*p <0.0001, \*\*p <0.001.

(F) Biallelic deletion of Enh2 (Enh2<sup>-/-</sup>) (~7kb) reveals no effect on the *Gtl2-Rian-Mirg* locus, whereas, biallelic deletion of IG-DMR/Enh1 (IG-DMR/Enh1<sup>-/-</sup>) (~7kb) abrogates expression of maternal *Gtl2*, *Rian* and *Mirg*. Non-Enh2<sup>-/-</sup> (~7kb) used as a control. mRNA expression of *Dlk1*, *Dio3*, *Gtl2*, *Rian* and *Mirg* were examined from undifferentiated wild-type, IG-DMR<sup>-/-</sup>, Enh2<sup>-/-</sup> and Non-Enh2<sup>-/-</sup> mESCs. mRNA expressions are represented as mean  $\pm$  SEM (n=3); p-values were calculated using a 2-way ANOVA; \*\*\*p <0.0001, \*\*p <0.001, \*p <0.01, ns (non-significant).

See also Figure S3.

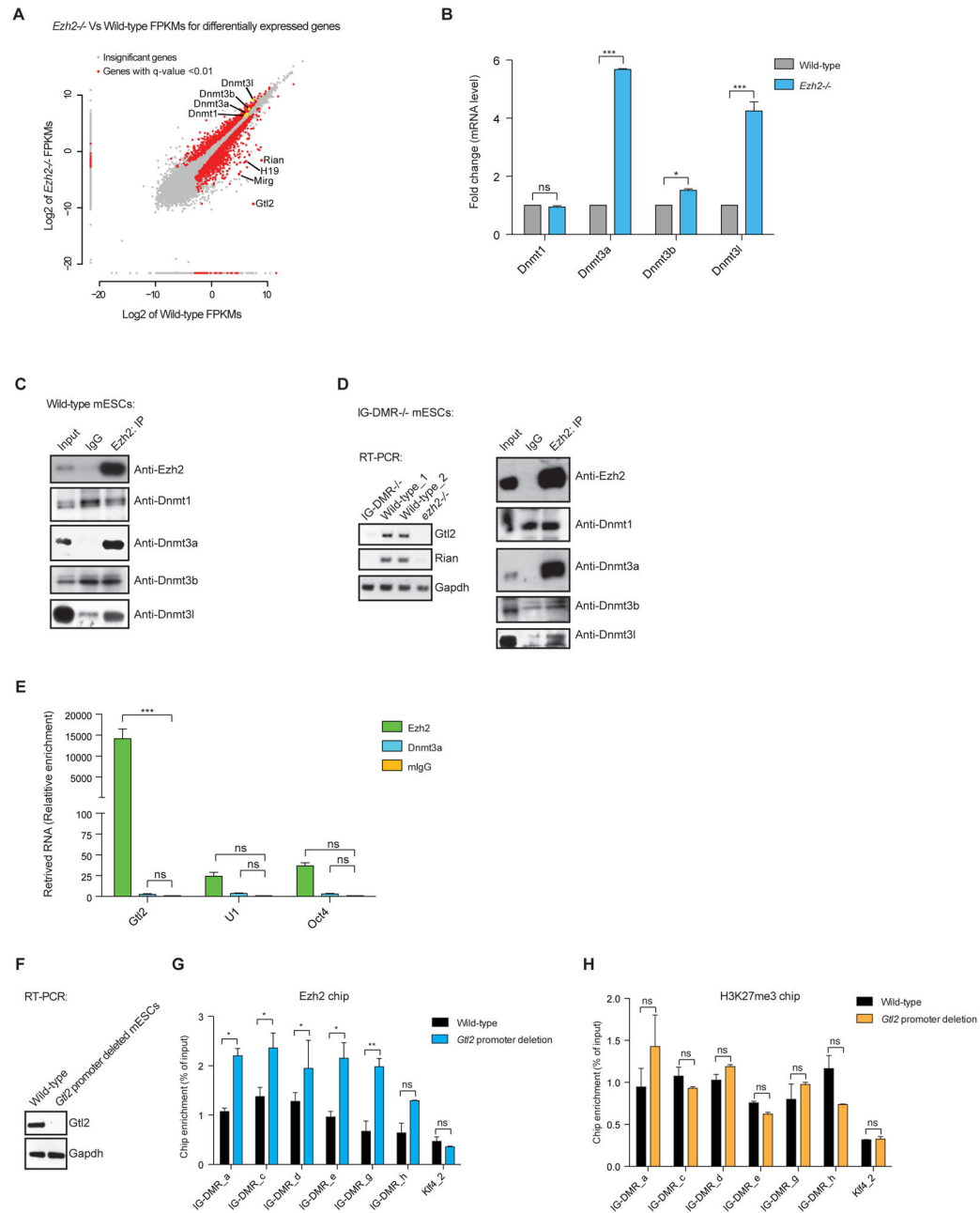


**Figure 4. PRC2 physically interacts with Dnmt3a/3l in Gtl2 lncRNA-independent manner; the interaction between Gtl2 lncRNA-Ezh2 inhibits binding of Ezh2/PRC2 at the IG-DMR** (A) Scatter plot representing differentially expressed genes from *Ezh2*<sup>-/-</sup> mESCs compared to wild-type. Red dots represents significantly up- and down-regulated genes in *Ezh2*<sup>-/-</sup> mESCs with a q-value < 0.01. Genes of interest are labeled in the scatter-plot. (B) mRNA expression shows significant up-regulation of Dnmt3a, Dnmt3b and Dnmt3l, but not Dnmt1, in *Ezh2*<sup>-/-</sup> mESCs as compared to wild-type. Transcript levels were normalized to Gapdh. Data are represented as mean  $\pm$  SEM (n=3); p-values were calculated using a 2-way ANOVA; \*\*\*p < 0.0001, \*p < 0.01, ns (non-significant).

- (C) Anti-Ezh2 antibody was used to immunoprecipitate endogenous Ezh2 from mESCs nuclear extracts, which shows a specific interaction between Ezh2 and Dnmt3a/Dnmt3l.
- (D) RT-qPCR shows that biallelic deletion of IG-DMR<sup>-/-</sup> causes abrogation of maternal Gtl2 and Rian lncRNAs in mESCs. Endogenous Ezh2 maintains interaction with Dnmt3a/Dnmt3l in absence of Gtl2 lncRNA.
- (E) RNA immunoprecipitation (RIP) demonstrates a strong interaction of Gtl2 lncRNA with Ezh2, but not with Dnmt3a. U1 RNA and Oct4 mRNA were used as controls. Data are represented as mean  $\pm$  SEM (n=3); p-values were calculated using a 2-way ANOVA; \*\*\*p <0.0001, ns (non-significant).
- (F) RT-qPCR shows that biallelic deletion of *Gtl2* promoter (~7kb) disrupts the formation of Gtl2 lncRNA.
- (G) ChIP-qPCR shows increased Ezh2 occupancy at the IG-DMR in absence of Gtl2 lncRNA. Data are represented as mean  $\pm$  SEM (n=3); p-values were calculated using a 2-way ANOVA; \*\*p <0.001, \*p <0.01, ns (non-significant).
- (H) ChIP-qPCR shows no significant increase binding of H3K27me3 at the IG-DMR in absence of Gtl2 lncRNA. Data are represented as mean  $\pm$  SEM (n=3); p-values were calculated using a 2-way ANOVA; ns (non-significant).
- See also Figure S4.



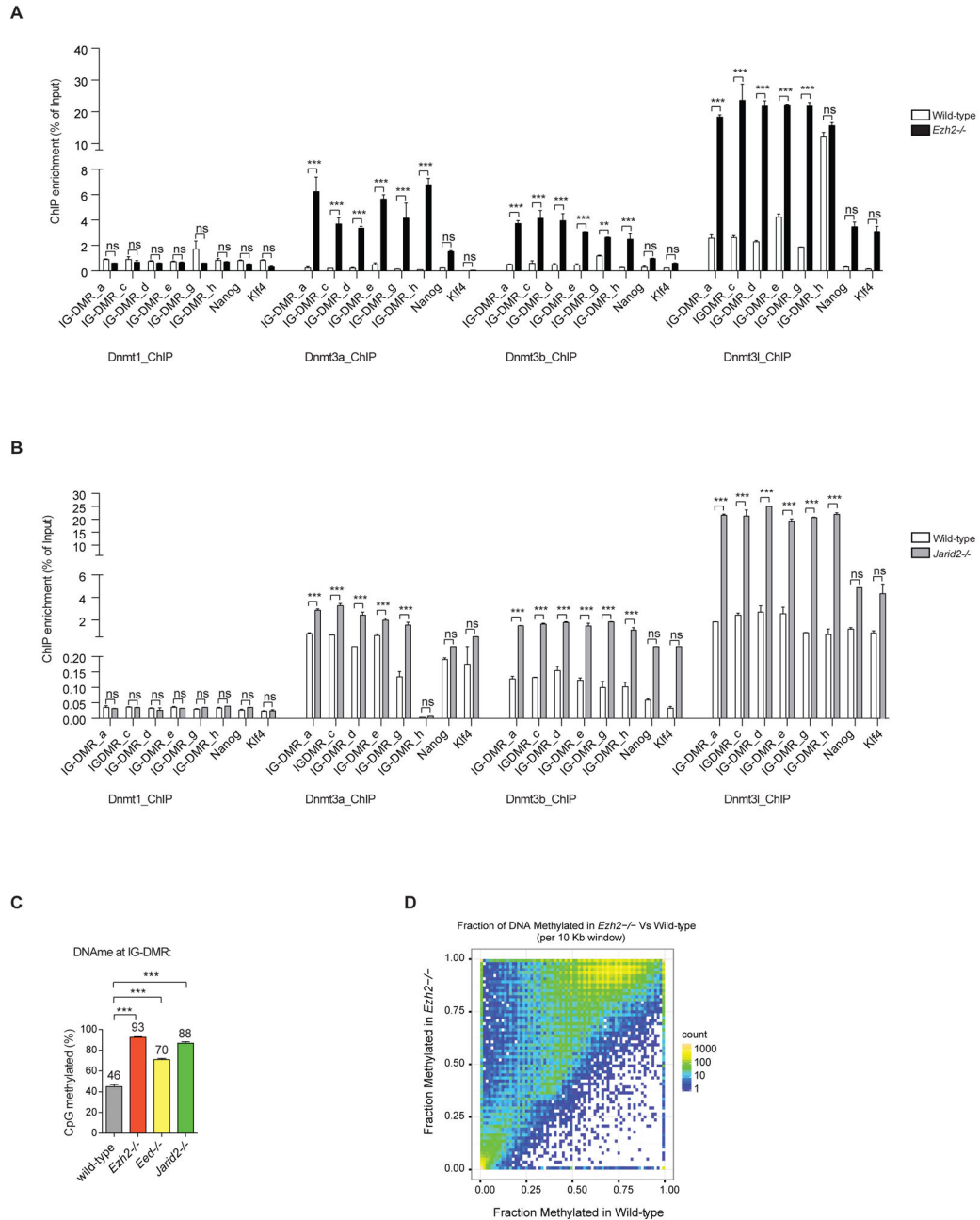


**Figure 5. PRC2 antagonizes *de novo* DNAm at the IG-DMR through distinct mechanism** (A–B) ChIP-qPCR shows Dnmt3a, Dnmt3b and Dnmt3l occupancy at IG-DMR is significantly increased in absence of Ezh2 and Jarid2, but occupancy of Dnmt1 remains unchanged. Data are represented as mean  $\pm$  SEM (n=3); p-values were calculated using a 2-way ANOVA; \*\*\*p < 0.0001, ns (non-significant). (C) Analysis of 29 CpGs at the IG-DMR shows different DNAm (%) levels in the absence of PRC2 components. Data are represented as mean  $\pm$  SEM (n=3); p-values were calculated using a 2-way ANOVA; \*\*\*p < 0.0001.

(D) Global DNA methylation (DNAm) analysis from *Ezh2*<sup>-/-</sup> and wild-type mESCs, using reduced-representation bisulfite sequencing (RRBS), represented as heat map of genome wide methylation patterns. The genome was divided into non-overlapping 10kb windows and the fraction of methylated CpGs in each window was computed for wild type and *Ezh2*<sup>-/-</sup> mutants. The hue represents the number of genomic windows with a given fractional methylation in *Ezh2*<sup>-/-</sup> vs wild-type. Trends suggest significantly increased global DNAmethylation in *Ezh2*<sup>-/-</sup>.  
See also Figure S5.

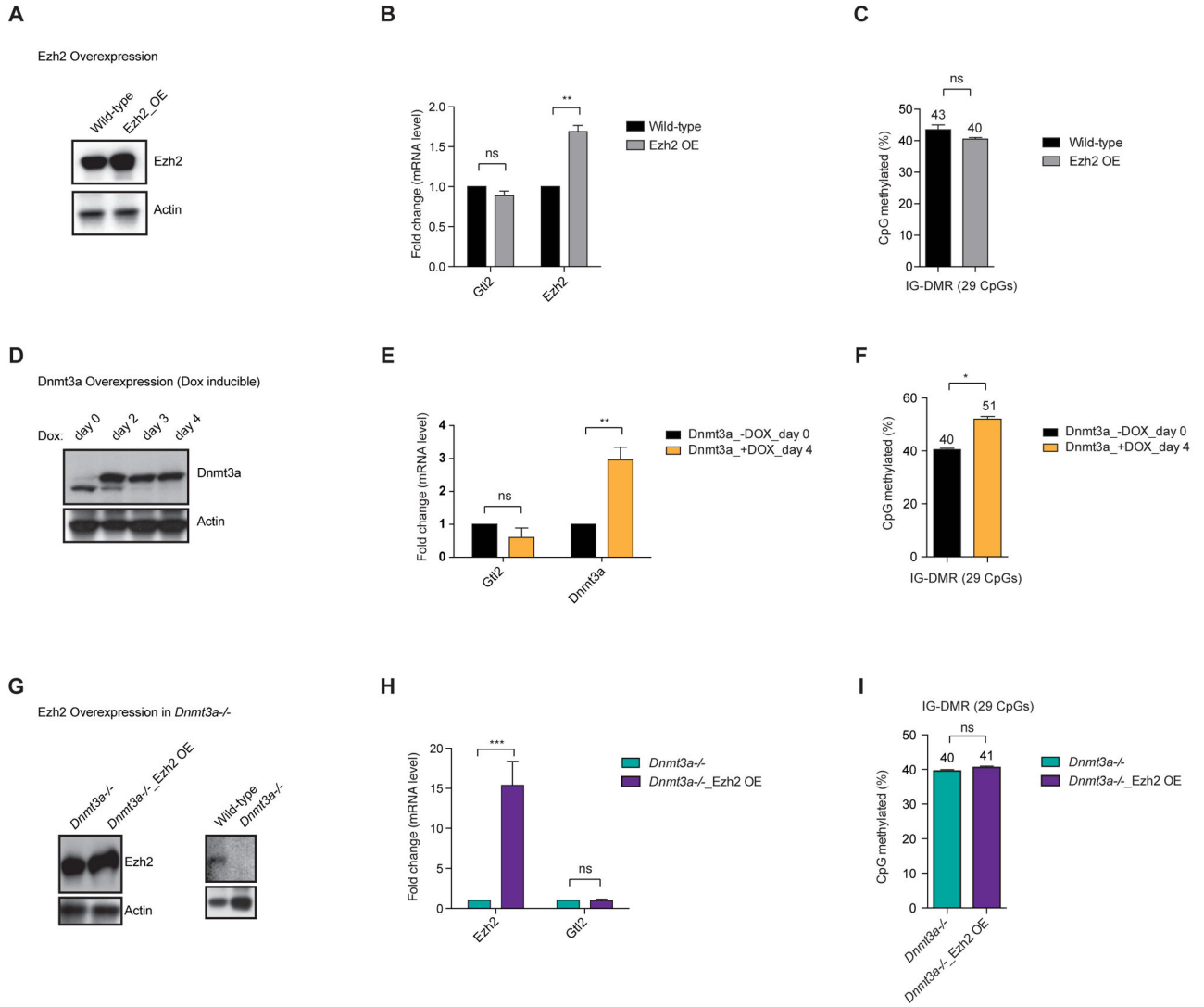


**Figure 6. PRC2 protects IG-DMR from *de novo* DNAm to allow proper expression of the maternal *Gtl2-Rian-Mirg* locus**

(A) Overexpression of Ezh2 in wild-type mESCs. Protein expression of Ezh2 was checked through western blot. Actin used as an internal control.

(B) mRNA expression shows no significant change of *Gtl2* lncRNA expression upon overexpression of Ezh2. Transcript levels were normalized to *Gapdh*. Data are represented as mean  $\pm$  SEM (n=3); p-values were calculated using a 2-way ANOVA; \*\*p < 0.001, ns (non-significant).

(C) Analysis of 29 CpGs at the IG-DMR shows no significant changes of DNAm (%) levels upon overexpression of Ezh2. Data are represented as mean  $\pm$  SEM (n=3); p-values were calculated using a 2-way ANOVA; ns (non-significant).

(D) Dox-inducible overexpression of Dnmt3a (western blot) does not change *Gtl2* lncRNA expression (RT-qPCR) (E), with slight increase of DNAm level at the IG-DMR (F). Data are represented as mean  $\pm$  SEM (n=3); p-values were calculated using a 2-way ANOVA; \*\*p < 0.001, ns (non-significant).

(G) Overexpression of Ezh2 in *Dnmt3a*<sup>-/-</sup> mESCs (western blot) leads to no significant change in Gtl2 lncRNA expression (RT-qPCR) (H) and DNAm at the IG-DMR (I). Data are represented as mean  $\pm$  SEM (n=3); p-values were calculated using a 2- way ANOVA; \*\*\*p <0.0001, ns (non-significant).

See also Figure S6.

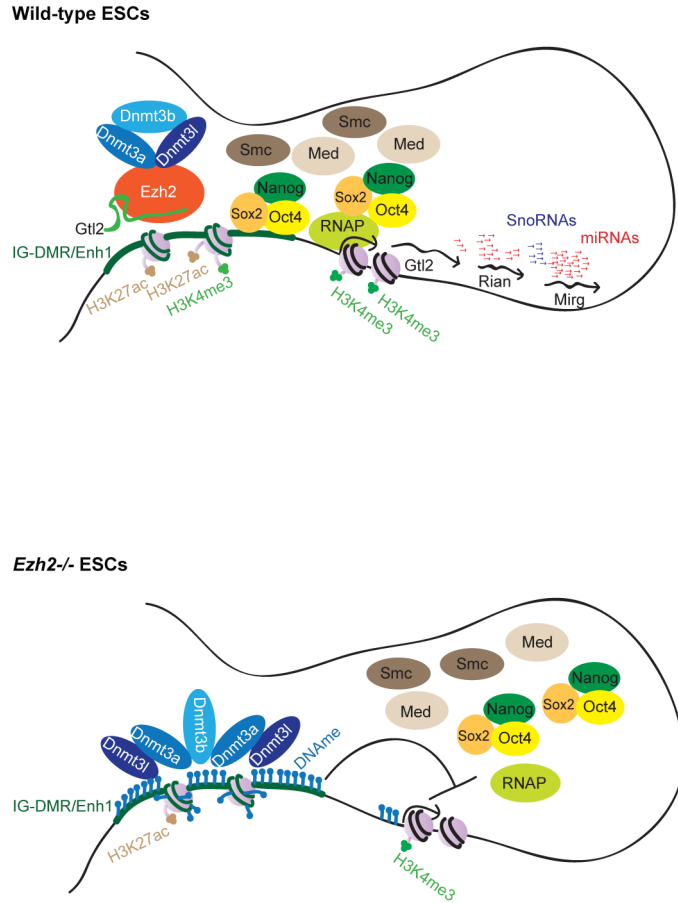


**Figure 7. The working model portrays the mechanism by which Ezh2/PRC2 protects the IG-DMR locus from *de novo* DNAm to allow proper expression of the maternal *Gtl2-Rian-Mirg* locus in mESCs**

A model schematically representing our findings, where Gtl2 lncRNA binds to Ezh2 and inhibits interaction of Ezh2/PRC2 at the IG-DMR locus, and subsequent deposition of H3K27me3. The presence of Ezh2/PRC2 in association with Gtl2 lncRNA prevents Dnmt3s recruitment and subsequent *de novo* DNAm, and allows ESC-specific TFs, mediators and other histone modifiers to bind at the IG-DMR/Enhancer1 locus that ultimately drives expression of the maternal *Gtl2-Rian-Mirg* locus. In the absence Ezh2, it is unable to prevent recruitment of Dnmt3s at the IG-DMR locus. Dnmt3s is then recruited to the IG-DMR and deposits *de novo* DNAm, leading to transcription repression of the maternal *Gtl2-Rian-Mirg* locus. Significant reduction of H3K27ac and H3K4me3 occupancy at the IG-DMR and *Gtl2* promoter is observed in the absence of Ezh2. For simplicity, only the maternal allele is shown.